Agricultural Water Management 96 (2009) 1293–1304

Contents lists available at ScienceDirect

Agricultural Water Management

journal homepage: www.elsevier.com/locate/agwat

Using ESAP software for predicting the spatial distributions of NDVI and transpiration of cotton

D.J. Hunsaker [a,*], D.M. El-Shikha [b], T.R. Clarke [a], A.N. French [a], K.R. Thorp [a]

[a] USDA-ARS, Arid Land Agricultural Research Center, Maricopa, AZ, USA
[b] Agricultural and Biosystems Engineering, University of Arizona, Maricopa, AZ, USA

ARTICLE INFO

Article history:
Received 23 October 2008
Accepted 12 April 2009

Keywords:
Remote sensing
Crop coefficients
Irrigation management
Crop water use

ABSTRACT

Observations of the normalized difference vegetation index (NDVI) from aerial imagery can be used to infer the spatial variability of basal crop coefficients (Kcb), which in turn provide a means to estimate variable crop water use within irrigated fields. However, monitoring spatial Kcb at sufficient temporal resolution using only aerial acquisitions would likely not be cost-effective for growers. In this study, we evaluated a model-based sampling approach, ESAP (EC_e Sampling, Assessment, and Prediction), aimed at reducing the number of seasonal aerial images needed for reliable Kcb monitoring. Aerial imagery of NDVI was acquired over an experimental cotton field having two treatments of irrigation scheduling, three plant density levels, and two N levels. During both 2002 and 2003, ESAP software used input imagery of NDVI on three separate dates to select three ground sampling designs having 6, 12, and 20 sampling locations. On three subsequent dates during both the years, NDVI data obtained at the design locations were then used to predict the spatial distribution of NDVI for the entire field. Regression of predicted versus imagery observed NDVI resulted in r^2 values from 0.48 to 0.75 over the six dates, where higher r^2 values occurred for predictions made near full cotton cover than those made at partial cover. Prediction results for NDVI were generally similar for all three sample designs. Cumulative transpiration (Tr) for periods from 14 to 28 days was calculated for treatment plots using Kcb values estimated from NDVI. Estimated cumulative Tr using either observed NDVI from imagery or predicted NDVI from ESAP procedures compared favorably with measured cumulative Tr determined from soil water balance measurements for each treatment plot. Except during late season cotton senescence, errors in estimated cumulative Tr were between 3.0% and 7.3% using observed NDVI, whereas they were they were between 3.4% and 8.8% using ESAP-predicted NDVI with the 12 sample design. Thus, employing a few seasonal aerial acquisitions made in conjunction with NDVI measurements at 20 or less ground locations optimally determined using ESAP, could provide a cost-effective method for reliably estimating the spatial distribution of crop water use, thereby improving cotton irrigation scheduling and management.
Published by Elsevier B.V.

1. Introduction

Frequent monitoring of remotely sensed vegetation indices in agricultural fields can provide important crop growth information for many precision agricultural applications (Pinter et al., 2003). Precision irrigation is a management approach that attempts to precisely match water application amounts to spatially distributed crop water use (Sadler et al., 2000). Such management techniques would be greatly enhanced by collection of timely and spatially contiguous data on crop evapotranspiration (ETc) within fields. A simple, yet promising, approach utilizes crop coefficients derived from the normalized difference vegetation index (NDVI) along with local climatic data to infer variable crop ETc quantities in near real-time (Hunsaker et al., 2005; Er-Raki et al., 2007; Gonzalez-Dugo and Mateos, 2008). Hunsaker et al. (2005) derived relationships to calculate the basal crop coefficient (Kcb) for cotton as a function of NDVI. Subsequently, Hunsaker et al. (2005) used frequent ground-based observations of NDVI and these relationships to estimate Kcb during field studies with cotton. Their results showed that the NDVI-based Kcb data, multiplied by grass-reference evapotranspiration obtained from a local meteorological station, provided reasonably good estimates of cotton transpiration (Tr) for guiding irrigation scheduling during the season. For applying this approach to the commercial field scale, the required remote sensing data for NDVI can be acquired from imagery aboard satellite (Moran et al., 1997) and aircraft (Wood et al., 2003; Fitzgerald et al., 2006). Pinter et al. (2003), as well as Trout et al.

* Corresponding author at: US Arid Land Agricultural Center, Maricopa, AZ 85238, USA. Tel.: +1 520 316 6372; fax: +1 520 316 6330.
E-mail address: doug.hunsaker@ars.usda.gov (D.J. Hunsaker).

0378-3774/$ – see front matter. Published by Elsevier B.V.
doi:10.1016/j.agwat.2009.04.014

(2008), however, cite several examples including cost, spatial resolution and frequency of data, and data availability that may limit the sufficiency of satellite and aircraft platforms for real-time, crop coefficient irrigation management.

Ground-based data collection consisting of radiometers or other sensors mounted on center pivot irrigation systems (Peters and Evett, 2007), tractors (Scotford and Miller, 2004), sprayers (Sui et al., 2008), or other moveable agricultural equipment are presently being developed for remote sensing monitoring during the growing season. While such systems could offer viable alternatives to aerial imagery in many instances, they would not be generally applicable for collecting frequent NDVI data within surface-irrigated fields. An alternative NDVI acquisition system envisioned for surface-irrigated fields is to implement a network of fixed, oblique viewing, radiometric sensors that collect daily data at certain locations within a field. For the network system to be cost effective, a minimum number of sensors should be employed within each field. However, the optimal locations for a small number of fixed sensors in a field would need to be identified. Ideally, the locations selected are those that would offer the best chance for statistically predicting the spatial patterns of NDVI within the entire field.

Grid-point and management zone sampling are two common techniques for acquiring field spatial variability information in precision agriculture (Chang et al., 2003). In the first approach, a sampling grid network is generally established at regular intervals within the field (Chang et al., 2003). In contrast, the management zone approach is based on the assumption that a field is a mosaic of different zones, where each zone has exclusive characteristics (Fleming et al., 2000). For this approach, samples are collected from each management zone. Using either of these techniques (or a combination of them) can be effective for small sample sizes, but they rapidly become impractical and costly for large sample sizes. Additionally, neither technique addresses the associated problem of spatial autocorrelation, a factor that degrades the performance of resulting regression equations (Fitzgerald et al., 2006).

One way that reduces these problems is to sample spatial variability of vegetation characteristics in a statistically optimal way. This sampling approach, developed by Lesch et al. (1995), Lesch et al. (2000), and Lesch (2005), considers the need to represent the full range of spatial variability while also minimizing sample sizes. The software package, EC_e Sampling, Assessment, and Prediction (ESAP), implements this approach by ensuring that samples are spatially representative for the entire survey region and by establishing empirical relationships between observations and estimates. ESAP was originally developed for generating optimal soil salinity sampling designs using bulk soil conductivity survey data (Lesch et al., 2000), but in principle can be used with various types of remotely sensed data, such as NDVI (Fitzgerald et al., 2006). ESAP is a spatial site selection algorithm specifically designed to identify calibration sites that are well suited for multiple linear regression models. The ESAP algorithms select a limited set of calibration sites (6, 12, or 20 sites) having desirable spatial and statistical characteristics by combining survey site location information with response surface design techniques. These regression models can in turn be used to predict the spatial values of the variable of interest across the field.

In this study, we used the ESAP algorithms to select NDVI sampling locations within an irrigated cotton field. A full set of field NDVI values (>17,000 pixels) acquired from aerial imagery on six days during two cotton growing seasons were applied in ESAP to select sample designs having 6, 12, and 20 locations. The primary objective was to test the ability of ESAP to successfully predict the field spatial distribution of NDVI on a subsequent date in the season using only NDVI data collected at the few sample locations. A secondary objective was to compare differences in NDVI prediction due to the number of sampling locations employed. A full set of observed NDVI data obtained from aerial imagery on the subsequent dates were used to evaluate the predictions. Thirdly, an evaluation was made to assess the effectiveness of using Kcb generated from ESAP-predicted NDVI data to estimate spatially variable measured Tr within the irrigated cotton field.

2. Materials and methods

2.1. Field description

Remote sensing irrigation scheduling experiments, previously described by Hunsaker et al. (2005), were conducted during two cotton seasons on a 1.3-ha field planted on April 22, 2002 (day of year [DOY] 112) and on April 16, 2003 (DOY 106) at The University of Arizona, Maricopa Agricultural Center (MAC). The soil was a Casa Grande series (Typic Natriargid, fine-loamy, mixed, hyperthermic) with a predominantly sandy loam texture. The experimental configuration was a randomized design with incomplete blocking that included 32 plots, each 11.2 m × 21 m. Three treatment factors were imposed in the experiments: irrigation scheduling protocol (i.e., Kcb method), plant density, and nitrogen level, resulting in 12 sub-treatments (Table 1). The configuration allowed testing of crop coefficient irrigation scheduling, while considering differences in cotton growth and ETc due to plant density and fertilization. The two irrigation scheduling treatments, equally divided into 16 plots each, were based on crop ETc estimates using a standard FAO-56 Kcb curve described by Allen et al. (1998) and denoted as the FAO Kcb method, and an NDVI-based Kcb approach (Hunsaker et al., 2005), denoted as the NDVI Kcb method. During these experiments, NDVI observations were obtained for all plots every few days using a hand-held radiometer. Plants were sown at three densities: 5, 10, and 20 plants/m^2, denoted as sparse, typical, and dense treatments, respectively. Nitrogen fertilizer was applied at two levels, designated high and low N treatments. For the 2002 experiment, the high and low treatments received ≈236 and ≈96 kg N/ha, respectively, whereas for 2003, they received ≈172 and ≈60 kg N/ha, respectively. The plots were hand-harvested in October 2002 and 2003.

Neutron scattering and time-domain-reflectometry (TDR) techniques were used to obtain frequent measurements of soil water contents for all 32 plots to a depth from 0 to 3.0 m below the soil surface. The soil water content data, collected near the center of each plot, were used along with measurements of irrigation volumes and rainfall, to calculate cumulative ETc during the season as the residual of the soil water balance equation. Hunsaker et al. (2005) presented and described the procedures used to obtain the separate cumulative Tr and soil evaporation components of the cumulative ETc. Measured daily meteorological data, including solar radiation, air temperature, wind speed, humidity, and rainfall were used to compute daily values for the grass-reference evapotranspiration (ETo) using the FAO-56 Penman–Monteith equation (Allen et al., 1998). The meteorological data were provided by the University of Arizona, AZMET weather station (Brown, 1989) that was located approximately 200 m from the field site.

2.2. Remote sensing imagery

Imagery was acquired from aircraft using a mounted Duncan-Tech camera[1] (MS3100; Redlake Inc., San Diego, CA) that obtained visible and near infrared (VNIR) imagery in three bands centered at 670, 720, and 790 nm with 10 nm bandwidths. The flight elevation in both years was about 800 m above ground level. The camera

[1] Mention of company or trade names does not imply endorsement by the USDA.

Table 1
Summary of sub-treatment variables for the 2002 and 2003 cotton experiments.

Sub-treatment acronym	Experimental variables			Number of replicates
	Kcb method	Plant density	Nitrogen level	
FSH	FAO (F)	Sparse (S)	High (H)	2
FSL	FAO (F)	Sparse (S)	Low (L)	2
FTH	FAO (F)	Typical (T)	High (H)	4
FTL	FAO (F)	Typical (T)	Low (L)	4
FDH	FAO (F)	Dense (D)	High (H)	2
FDL	FAO (F)	Dense (D)	Low (L)	2
NSH	NDVI (N)	Sparse (S)	High (H)	2
NSL	NDVI (N)	Sparse (S)	Low (L)	2
NTH	NDVI (N)	Typical (T)	High (H)	4
NTL	NDVI (N)	Typical (T)	Low (L)	4
NDH	NDVI (N)	Dense (D)	High (H)	2
NDL	NDVI (N)	Dense (D)	Low (L)	2

field of view was $15^\circ \times 20^\circ$ and the pixel resolution for the experiments was ≈0.5 m. Imagery was acquired about 60–90 min after solar noon, between 13:15 and 14:00 h, local time. The VNIR data were calibrated using four, 8 m × 8 m standard reflectance tarps placed near the field having nominal reflectances of 4%, 8%, 48%, and 64% (Fitzgerald et al., 2006). Image processing, including geo-registration and masking, was performed using IMAGINE^2 software (Version 9.1; ERDAS, Inc., Atlanta, GA). Raw imagery was first converted to reflectance (ρ) and then to NDVI using Eq. (1):

$$\text{NDVI} = \frac{\rho_{790} - \rho_{670}}{\rho_{790} + \rho_{670}} \quad (1)$$

IMAGINE^2 software was also used to delete any reflectance data obtained for the soil border dikes between treatment plots as well as that outside of the field's boundary.

Ten dates of imagery collection were considered in this study, which were divided into two sets. Survey imagery, denoted as Set A, included imagery obtained on six different dates over the two-year experiment: day of year (DOY) 163, 226, and 246 in 2002, and DOY 153, 176, and 190 in 2003. Calibration/prediction images, denoted as Set B, also included six dates: DOY 176, 246, and 261 in 2002, and DOY 168, 190, and 217 in 2003.

2.3. ESAP-software

The ESAP-95 Version 2.35R software package used in this study is public domain software developed by the USDA-ARS, George E. Brown, Jr., Salinity Laboratory (Lesch et al., 2000). The software contains three programs: ESAP-RSSD (Response Surface Sampling Design), designed to generate optimal sampling locations from survey data; ESAP-Calibrate, designed to estimate calibration equations to ultimately predict the spatial values of the desired variable from the survey data; and ESAP-SaltMapper, which produces high quality graphical outputs for survey and/or prediction data. All three programs were used in this study. The following sections describe the ESAP procedures that were employed. A flowchart provides a diagrammatic representation of the procedures (Fig. 1).

2.3.1. ESAP-RSSD (Response Surface Sampling Design)

The ESAP-RSSD is a statistical program that creates optimal sampling designs from survey information. The program uses a modified response surface sampling designed to statistically select a small set of sample locations from the survey data. Given the additional assumption of residual normality, the program optimizes parameters via least squares regression, while minimizing spatial correlation effects in the regression model residuals. The program does this by using an iterative algorithm to select adjacent sample locations as far apart as possible. The survey data are first transformed, de-correlated, and validated within the ESAP-RSSD program. The software uses a principle components analysis to de-correlate the survey data (e.g., when more than one signal reading is acquired at each site) and to identify and remove any outliers. ESAP then generates a set of optimal sample locations. More detailed information about the statistical methodology and algorithms used in the ESAP-RSSD program is given by Lesch (2005).

The primary goal of ESAP-RSSD is to select an optimal set of geo-registered locations from which the crop or soil attribute of interest will be sampled. The attribute data collected from the set of sample locations can then be used in ESAP-Calibrate to estimate calibration models for predicting individual site attributes within the field. ESAP provides the option of selecting 6, 12, or 20 calibration locations. For this study, NDVI aerial survey images (Set A) of the field collected on six dates spanning early to late season cotton growing periods were used (Table 2). ESAP-RSSD was applied to select 6, 12, and 20 NDVI calibration sites for each of the Set A image dates.

2.3.2. ESAP-Calibrate

The ESAP-Calibrate program is designed to use survey data and co-located calibration sample data to predict the spatial distribution of a particular soil or plant property, which for this study is NDVI. The software does this by first estimating a regression model, based on NDVI data acquired at the calibration locations,

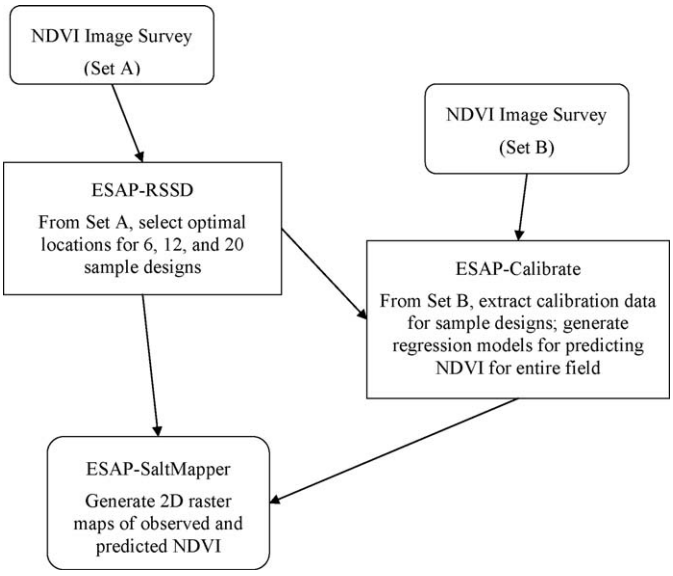

Fig. 1. Flowchart showing sequence of steps used in ESAP procedures.

Table 2
Dates of aerial images (Set A) used as survey data to select NDVI sample locations, which were used to calibrate and then predict the spatial NDVI for the entire field on a subsequent date (Set B). General conditions describe the growing period from Set A to Set B.

Set A (Survey)		Set B (calibrated/predicted)			General cotton field conditions
DOY	Year	NDVI[a]	DOY	Year	
163	2002	0.23	176	2002	35–50% ground cover; high N plots fertilized, DOY 155
226	2002	0.86	246	2002	80–100% ground cover; final irrigations, DOY 235
246	2002	0.79	261	2002	Late season senescence
153	2003	0.15	168	2003	25–40% ground cover; high N plots fertilized, 143–149
176	2003	0.56	190	2003	60–80% ground cover; high N plots fertilized, DOY 185–199
190	2003	0.69	217	2003	80–100% ground cover

[a] Indicates the field mean NDVI on the day of the survey image.

and then uses the model to generate NDVI predictions across the entire field. Additionally, the regression model can be used to create various field summary statistics, such as the average level of the target property in the field and the fractional area of the field that exhibits property values above a given threshold (referred to in ESAP as a "range interval estimate (RIE)").

After ESAP-RSSD identifies optimal locations within each sample design (i.e., 6, 12, and 20 locations) from a given NDVI survey image (Set A), the NDVI values at the corresponding geo-referenced sample locations were extracted from a subsequent image (Set B), occurring between 13 and 27 days later (Table 2). These NDVI values were then used to develop a calibration model to predict NDVI at all locations for the subsequent date. Note that in a practical application of this approach, perhaps only a few field survey images would be available to a grower during a cotton season. Thus, to predict point-to-point NDVI values for all field locations or field mean NDVI for another date after an image, the grower would need to collect ground-based NDVI at only the selected sample locations identified using ESAP procedures.

In the present approach, survey images for the six different dates during the cotton seasons (Set A, Table 2) provided NDVI values for over 17,000 locations within the field from which ESAP selected the calibration locations for the 6, 12, and 20 sample designs. A linear regression calibration model (Eq. (2)) was then fit using NDVI values for the selected calibration locations on the subsequent date (Set B) plus the full set of NDVI readings for the prior survey date (Set A).

$$\mathrm{NDVI} = b0 + b1(Z1) + \varepsilon \quad (2)$$

where NDVI is the measured NDVI value at a calibration location on the subsequent date, $b0$ and $b1$ are the regression intercept and slope coefficients, respectively, and $Z1$ is equal to the NDVI value at the location on the prior survey date minus the mean NDVI for the full set of NDVI readings on the survey date, divided by the standard deviation (SD) of NDVI on the survey date (Lesch et al., 2000). The effects of spatially correlated calibration model residuals were tested by the Moran score (I_{MS}) for each model, as calculated during the ESAP-Calibrate procedures (Lesch et al., 2000). The calibration regression model derived for each date (with Eq. (2)) was then used to predict the NDVI for all locations in the field on the subsequent date (i.e., Set B, Table 2). For example, survey data on DOY 163, 2002, were used to select calibration locations for calibration and prediction of NDVI for the entire field on DOY 176, 2002 (Table 2). Predicted NDVI field averages and range interval estimates were then compared with the full set of NDVI data from images acquired on the subsequent date. The performance of the prediction models were evaluated by the mean, SD, coefficient of determination (r^2), and the root mean square error (RMSE). Output (NDVI prediction) files created by the ESAP-Calibrate software were then imported into the ESAP-SaltMapper program.

2.3.3. ESAP-SaltMapper

The ESAP-SaltMapper program is designed to rapidly create 2D spatial raster maps of the target soil or plant property predictions. This program also contains an output ASCII text file feature which allows the prediction data file to be exported as a generic ASCII text file (for use in more sophisticated mapping software applications, such as Surfer or ArcGIS). For this study, the ESAP-SaltMapper program was used to generate the final 2D raster maps of the observed and predicted NDVI data.

2.4. Transpiration estimation

Data for NDVI obtained from imagery and ESAP predictions were also used to estimate basal crop coefficients. The NDVI-based Kcb were then used to calculate daily crop transpiration at the specific locations within each of the 32 treatment plots where soil water balance measurements were made. The approach involved, first, estimating daily Kcb values for the specific plot locations from NDVI and then multiplying the Kcb by ETc for the corresponding day, obtaining daily Tr. The Kcb were estimated using the two relationships presented by Hunsaker et al. (2005), in their Fig. 3, which derive the cotton Kcb as a function of NDVI.

Calculation of estimated Tr was considered separately for each of the six intervals summarized in Table 2, where the first day of an interval began on the DOY corresponding to the Set A image acquisition and the last day of the interval occurred on the DOY of the subsequent Set B image acquisition. For example, the interval between DOY 163 and 176 in 2002 included 14 days of calculated Tr for each location, whereas the interval between DOY 190 and 217 in 2003 included 28 days. For all six intervals, the actual imagery observation of NDVI (i.e., from the Set A image) for each of the 32 specific plot locations was used for the location's NDVI on the first day of the interval. The predicted NDVI values for each location obtained using the ESAP procedures for the 6, 12, and 20 sample designs were used as the location's NDVI on the last day of the interval. For comparison, calculation of estimated Tr for each interval was also made using the observed NDVI for each location (i.e., obtained from the Set B image) as the location's NDVI on the last day of the interval. For each location, the daily NDVI values for the entire interval were obtained by linear interpolation between the location's first and last NDVI values for the interval.

For each of the 32 treatment plot locations, the daily Kcb were calculated as a function of the daily NDVI using either the primary function, valid from planting until cotton cutout, or the late season function, used after cutout, as described by Hunsaker et al. (2005). The late season function was used for days occurring after cutout (DOY 241) for calculating Kcb in 2002 (i.e., it was used for a few final days for the interval from 226 to 246, and for all days for the interval from DOY 246 to 261). Cutout occurred on DOY 235 in 2003 and, therefore, the late season function was not used for any of the 2003 intervals, which included only days before DOY 235. After determining daily Kcb from NDVI, it was multiplied by the

corresponding ETc for each day, obtaining daily Tr values for each day in the interval. The daily Tr were then summed over all days within the interval to obtain the cumulative Tr. This was done for each of the 32 treatment plot locations.

The calculated cumulative Tr for each plot was compared to the cumulative Tr obtained as a residual from the soil water balance measurements made for each plot. Statistical analyses were made to evaluate agreement between estimated cumulative Tr and the cumulative Tr from the soil water balance. Statistical evaluation parameters included the coefficient of determination (r^2), root mean square error (RSME), mean absolute error (MAE) (Legates and McCabe, 1999), and mean absolute percent difference (MAPD) (Kustas et al., 1999).

3. Results and discussion

3.1. NDVI prediction

Fig. 2 shows the selected NDVI calibration locations that were used to predict the spatial distribution of NDVI for the cotton field on DOY 176 (2002). The sites for the 6, 12, and 20 sample schemes (indicated by ID reference numbers on the map) were determined from ESAP-RSSD using survey data for DOY 163, 2002. Note that several of the locations selected for each sample scheme were close to the outer edges of the field. As mentioned earlier, ESAP-RSSD attempts to locate sites as far apart as possible to minimize spatial autocorrelation in the regression model residuals. The 12 and 20 sample schemes also had several common calibration locations selected by ESAP.

Regression model summary statistics obtained for the 6, 12, and 20 sample designs are shown in Table 3a, b, and c, respectively, for each of the six calibration/prediction dates. Although the linear regression models obtained for each date and sample scheme were significant at a probability of 0.05 or less, model r^2 values varied considerably (0.51–0.96), as did the RMSE, 0.034–0.103. With one exception, model I_{MS} scores were not significant, which indicates the assumption of spatial independence was not violated. The significant I_{MS} for the 20 location scheme on DOY 176 (Table 3c) suggests that predictions of NDVI for field locations with that model could be biased.

The regression calibration models that were estimated for predicting DOY 176, 2002 and DOY 168, 2003 had generally lower r^2 values and higher RMSE compared to models estimated at later dates during the growing seasons (Table 3). Calibration locations for DOY 176 and DOY 168 were selected from survey data on DOY 163, 2002 and DOY 153, 2003, when the mean NDVI for the field were 0.23 and 0.15, respectively (Table 2). Most likely, less efficient calibration models occurred during the earlier season conditions because NDVI was more highly influenced by soil background. At later times during the season, larger cotton canopies reduced the effects of soil background on NDVI. Considering r^2 and RMSE values, it appeared that prediction models for the sample designs containing 6 and 12 locations were as robust as those for the 20 location design (Table 3).

The observed and ESAP-predicted NDVI means calculated using over 17,000 points for the entire field are shown for all six prediction dates in Table 4a, b, and c, respectively, for the 6, 12, and 20 sample designs. The difference between predicted and observed means were less than 3%, except on DOY 176, 2002 which varied from 5% to 17% for the three sample designs. However, for all cases, the predicted means were statistically equal to the observed means at the 95% confidence level. Thus, the ESAP calibration models for all three sample designs appeared to provide reasonably good estimates of field-wide NDVI means. The lower standard deviation of NDVI for predicted than observed NDVI does suggest, however, that the models were not effective in predicting the upper and lower extremes of the observed NDVI.

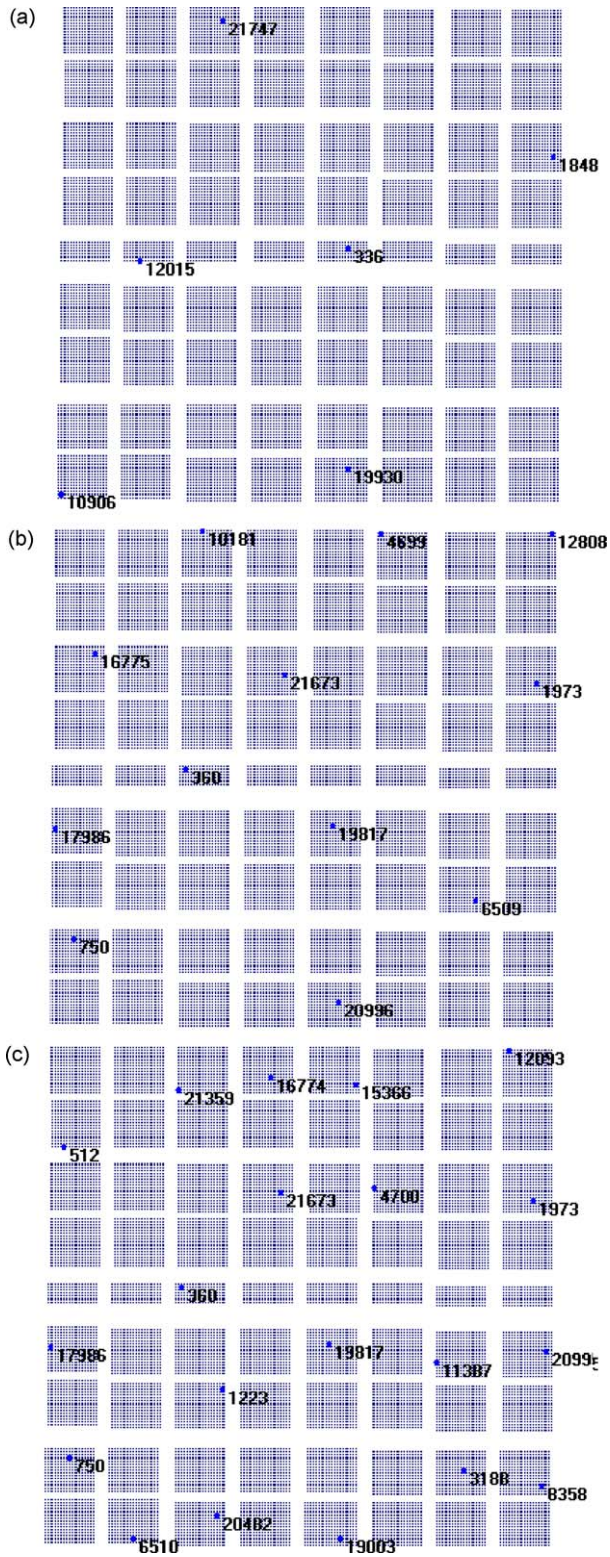

Fig. 2. Selected sample locations as output from ESAP-RSSD from survey data on DOY 163, 2002, for prediction of NDVI on DOY 176 for (a) 6, (b) 12, and (c) 20 sample locations designs.

Comparison of the three sample designs in Table 4 shows that the prediction r^2 values were the same for all designs for a given date, though RMSE values varied somewhat among the designs. Similar to the seasonal r^2 trends for calibration models (Table 3),

Table 3
Regression model statistics for the six calibration/prediction dates using (a) 6, (b) 12, and (c) 20 sample locations selected in ESAP-RSSD. Regression coefficients, $b0$ and $b1$, are the intercept and slope, respectively, r^2 is the coefficient of determination, and RMSE is the root mean square error. I_{MS} Prob is the significance level of the Moran test for spatial independence of regression residuals.

DOY	Year	Regression coefficients		r^2	RMSE	I_{MS} Prob
		$b0$	$b1$			
(a)						
176	2002	0.343	0.075	0.67	0.090	0.277
246	2002	0.775	0.113	0.93	0.034	0.216
261	2002	0.717	0.111	0.79	0.065	0.888
168	2003	0.385	0.089	0.76	0.103	0.136
190	2003	0.699	0.132	0.96	0.050	0.264
217	2003	0.873	0.071	0.86	0.050	0.521
(b)						
176	2002	0.388	0.086	0.70	0.077	0.541
246	2002	0.772	0.108	0.89	0.037	0.697
261	2002	0.751	0.088	0.86	0.034	0.162
168	2003	0.381	0.068	0.66	0.068	0.137
190	2003	0.700	0.121	0.95	0.045	0.889
217	2003	0.888	0.056	0.73	0.051	0.554
(c)						
176	2002	0.378	0.076	0.56	0.089	0.019
246	2002	0.781	0.111	0.51	0.079	0.464
261	2002	0.764	0.101	0.81	0.045	0.583
168	2003	0.360	0.113	0.83	0.071	0.580
190	2003	0.713	0.088	0.74	0.074	0.848
217	2003	0.878	0.064	0.66	0.062	0.482

the lowest prediction r^2 values occurred for early season dates, where the r^2 were 0.48 for DOY 176, 2002 and 0.55 for DOY 168, 2003 (Table 4). For all other dates, the r^2 were 0.63–0.88. As noted earlier, less efficient calibration models were obtained for the early season conditions. However, the lower prediction r^2 values for DOY 176 and 168 may also suggest that the spatial structure for NDVI during the early season was less stable between the time the survey was made and the subsequent prediction than for later seasonal periods. That is, the spatial stability of NDVI from point to point within the field was potentially disrupted to a greater extent due to crop management differences that occurred for treatment plots during the early season. Once plots approached full cover and maximum NDVI, the effects of treatment differences on NDVI were diminished and had a lesser impact on NDVI structure. As the prediction r^2 values increased from early to later seasonal conditions, the RMSE generally decreased (Table 4). Over all dates and sample designs, the RMSE varied from 0.030 to 0.076. Analysis and discussion of the NDVI predictions on the crop coefficients and Tr estimations will be addressed in the next section.

The ESAP-generated range interval estimates shown in Table 5 (2002) and Table 6 (2003) provide a means to compare how well the different sample designs predicted the observed variability of NDVI within the field. Note that an RIE represents the fraction of NDVI pixels falling within a specific interval range. For example, on DOY 176, 2002 (Table 5a), only 2.8% of the field had observed NDVI values below 0.2, whereas 42.9% of the field exhibited NDVI values between 0.2 and 0.4, etc. For DOY 176, 2002, the predicted RIE between 0.2 and 0.4 for the six sample design (76.6%) was much larger than the observed, whereas between 0.4 and 0.6 it was considerably smaller (21.4% versus 51.2%). On that particular early season date, observed RIE were somewhat better represented for the 12 or 20 than the six sample design. Overall RIE agreement was generally better for DOY 246 and 261, 2002 (Table 5b and c, respectively), as well as for all dates in 2003 (Table 6) compared to results for DOY 176. However, it was apparent that the predicted values of NDVI did not agree well with the observed NDVI for the 0–0.2-interval range. For all six prediction dates, a relatively stable

Table 4
Mean and standard deviation (SD) of NDVI for observed and ESAP-predicted, regression coefficient of determination (r^2) and root mean square error (RMSE) for predicted versus observed of the six calibration/prediction dates using (a) 6, (b) 12, and (c) 20 sample location designs.

DOY	Year	Observed		Predicted		r^2	RMSE
		Mean	SD	Mean	SD		
(a)							
176	2002	0.41	0.101	0.34	0.075	0.48	0.054
246	2002	0.77	0.158	0.77	0.113	0.84	0.045
261	2002	0.74	0.142	0.72	0.111	0.88	0.037
168	2003	0.37	0.127	0.38	0.089	0.55	0.059
190	2003	0.69	0.150	0.70	0.132	0.75	0.066
217	2003	0.89	0.132	0.87	0.071	0.63	0.043

DOY	Year	Observed		Predicted		r^2	RMSE
		Mean (SD)	SD	Mean	SD		
(b)							
176	2002	0.41	0.101	0.39	0.086	0.48	0.062
246	2002	0.77	0.158	0.77	0.108	0.84	0.043
261	2002	0.74	0.142	0.75	0.088	0.88	0.030
168	2003	0.37	0.127	0.38	0.068	0.55	0.047
190	2003	0.69	0.150	0.70	0.121	0.75	0.060
217	2003	0.89	0.132	0.89	0.057	0.63	0.034

DOY	Year	Observed		Predicted		r^2	RMSE
		Mean	SD	Mean	SD		
(c)							
176	2002	0.41	0.101	0.38	0.076	0.48	0.055
246	2002	0.77	0.158	0.78	0.111	0.84	0.044
261	2002	0.74	0.142	0.76	0.101	0.88	0.034
168	2003	0.37	0.127	0.36	0.113	0.55	0.076
190	2003	0.69	0.150	0.71	0.087	0.75	0.044
217	2003	0.89	0.132	0.88	0.064	0.63	0.039

portion (2–4%) of the observed total pixel area corresponded to NDVI values less than 0.2. The existence of these lower NDVI values was due to exposed patches of bare soil areas within the field. Although the amounts of bare soil pixels were small, their occurrence ultimately caused a slight bimodal distribution of observed NDVI rather than the normal distribution assumed in ESAP. The bimodal effects due to bare soil are depicted by the observed NDVI histograms for DOY 176, 2002 (Fig. 3a) and DOY

Table 5
Observed and predicted NDVI ratio interval estimates (RIE) for the 6, 12, and 20 sample designs on (a) DOY 176, (b) DOY 246, and (c) DOY 261 in 2002.

NDVI Intervals	Observed RIE (%)	Predicted RIE (%)		
		6	12	20
(a)				
0.0–0.2	2.81	1.94	1.14	0.80
0.2–0.4	42.9	76.6	57.4	63.1
0.4–0.6	51.2	21.4	39.9	35.6
0.6–0.8	3.07	0.04	1.50	0.43
0.8–1.0	0.00	0.00	0.00	0.00
(b)				
0.0–0.2	2.93	1.45	0.62	0.91
0.2–0.4	1.23	1.88	2.69	2.41
0.4–0.6	4.67	1.10	1.04	1.00
0.6–0.8	36.7	37.5	42.6	32.2
0.8–1.0	54.5	58.1	53.0	63.4
(c)				
0.0–0.2	2.63	0.10	0.00	0.00
0.2–0.4	0.77	3.33	2.17	2.89
0.4–0.6	6.46	5.31	2.32	1.69
0.6–0.8	53.4	76.8	65.8	49.9
0.8–1.0	36.8	14.4	29.7	45.6

Table 6
Observed and predicted NDVI ratio interval estimates (RIE) for the 6, 12, and 20 sample designs on (a) DOY 168, (b) DOY 190 and (c) DOY 217 in 2003.

NDVI intervals	Observed RIE (%)	Predicted RIE (%)		
		6	12	20
(a)				
0.0–0.2	4.16	0.45	0.04	4.67
0.2–0.4	67.8	62.3	65.9	63.6
0.4–0.6	18.7	35.6	33.8	28.5
0.6–0.8	9.30	1.64	0.24	3.17
0.8–1.0	0.00	0.00	0.00	0.01
(b)				
0.0–0.2	2.25	0.00	0.00	0.00
0.2–0.4	2.19	2.41	2.20	0.01
0.4–0.6	14.9	19.4	16.8	9.29
0.6–0.8	61.8	56.9	61.1	74.2
0.8–1.0	18.9	21.3	20.0	16.5
(c)				
0.0–0.2	1.92	0.00	0.00	0.00
0.2–0.4	0.38	0.00	0.00	0.00
0.4–0.6	0.89	1.58	0.00	0.01
0.6–0.8	4.07	9.73	5.88	8.64
0.8–1.0	92.8	88.7	94.1	91.3

190, 2003 (Fig. 3b). Because the predicted NDVI distributions are constructed in ESAP assuming normality of the survey data, distributions for the predicted NDVI are ultimately more symmetrical and of narrower range than the observed counterpart. This is illustrated by the histograms of predicted NDVI for the 12 sample location design on DOY 176 (Fig. 3c) and DOY 190 (Fig. 3d).

3.2. Transpiration estimation

The means of the 12 experimental sub-treatments (as defined in Table 1) for measured cumulative Tr are shown for each of the three intervals of 2002 (Fig. 4) and 2003 (Fig. 5). The sub-treatment means for estimated cumulative Tr, based on observed NDVI from imagery, are also presented in the figures for comparison with the measured data. Estimated Tr using the actual observed NDVI are presented since they give an indication of the best-case agreement with the measured Tr that can be expected when calculating Tr using the NDVI-based crop coefficient approach.

Treatments for high and low N applications started on DOY 155 in the 2002 cotton experiment, whereas irrigation treatments were not imposed until DOY 168. In Fig. 4a, differences for measured cumulative Tr between irrigation and N treatments during the early season interval of 2002 (DOY 163–176) were not apparent. However, the measured cumulative Tr was related to the differences in early-season plant canopy size, where measured Tr increased from the sparse to the dense treatments. The measured Tr trend due to plant density was estimated reasonably well for that interval, though estimated cumulative Tr was generally lower than the measured Tr for treatments (Fig. 4a). As the 2002 season progressed, differential irrigation scheduling resulted in less frequent irrigation for the NDVI than for the FAO treatment. The result was that greater soil water deficits occurred for NDVI than the FAO counterpart treatment (Hunsaker et al., 2005). The effects of the irrigation treatment differences on the measured cumulative Tr can be observed for the interval from DOY 226–246 (Fig. 4b), which shows reduced measured Tr for NDVI relative to its FAO sub-treatment counterpart (e.g.,

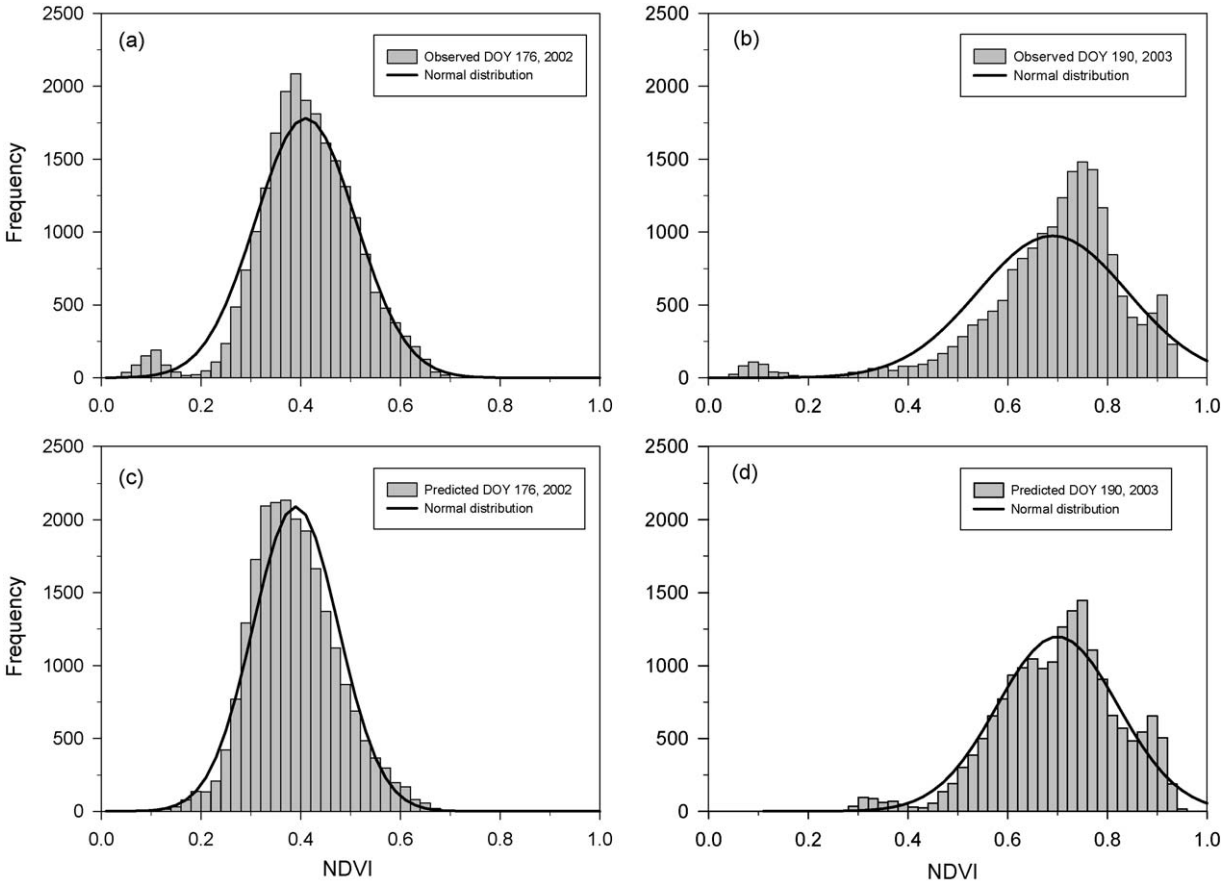

Fig. 3. Histograms for observed NDVI data and corresponding theoretical normal distribution functions on (a) DOY 176, 2002 and (b) DOY 190, 2003 compared with the histograms for predicted NDVI data and normal distribution functions for the 12 location sample design on (c) DOY 176, 2002 and (d) DOY 190, 2003.

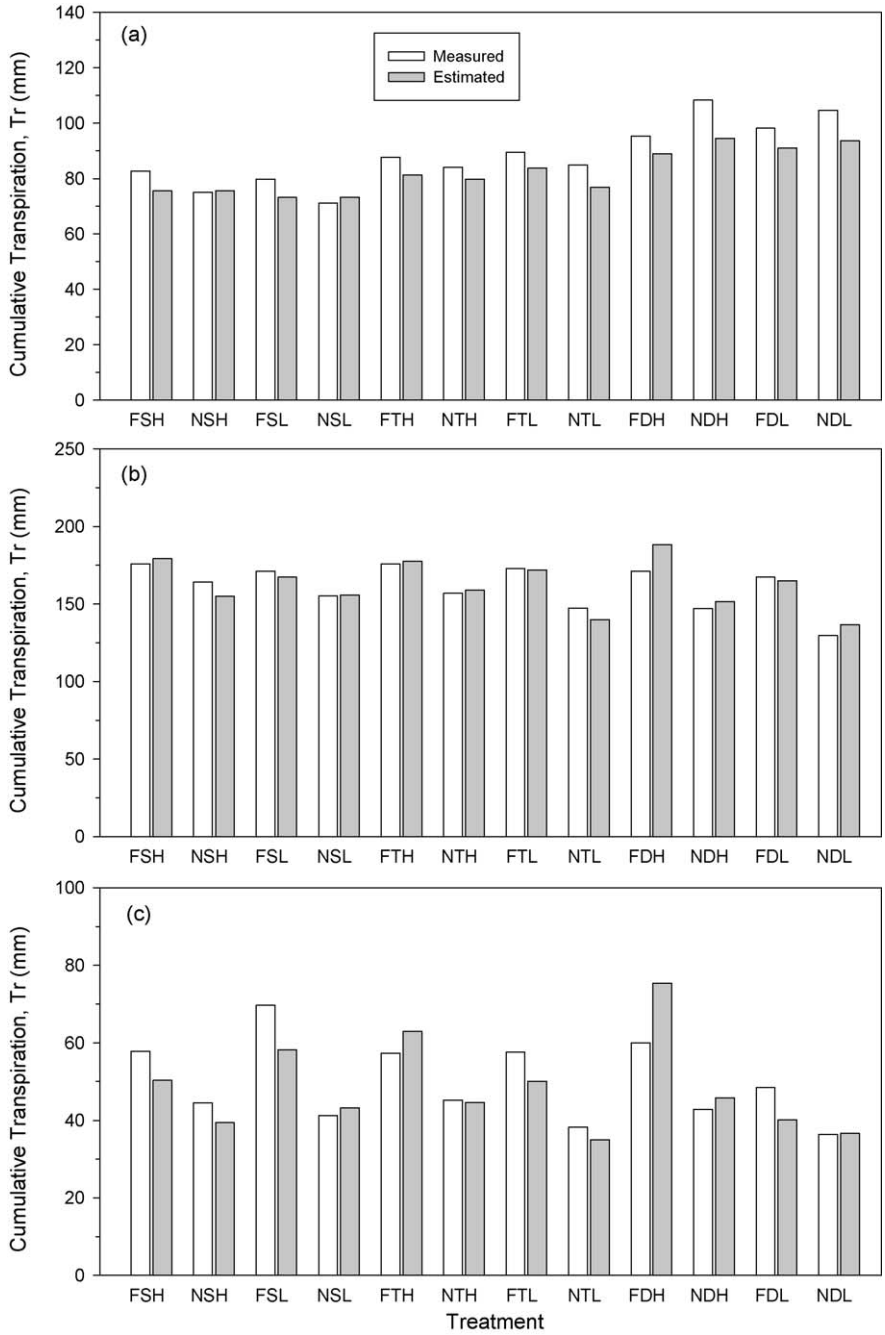

Fig. 4. Means for measured and estimated cumulative transpiration (Tr) for 12 treatments determined for intervals from (a) DOY 163–176, (b) DOY 226–246, and (c) DOY 246–261 in 2002. Measured Tr was determined from soil water balance measurements. Estimated Tr was obtained by multiplying daily Kcb values, derived from imagery-observed NDVI, by daily ETc for all days in a given interval.

comparison of NTH with FTH). The estimated cumulative Tr for the interval appeared to be in good agreement with the measured Tr (Fig. 4b). The last interval evaluated for 2002 was from DOY 246–261 (Fig. 4c) and all days in the interval occurred after cotton cutout. For this late season interval, the effects due to irrigation treatment on measured Tr were still apparent. However, the measured Tr was also related to nitrogen treatments, where measured Tr was, in many cases, lower for the low N versus the high N counterparts, particularly for the NDVI sub-treatments (e.g., NDL versus NDH). Since the late season interval occurred after cutout, the calculated Tr was based on the late season Kcb versus NDVI function, described earlier. The estimated cumulative Tr for the interval showed the general measured Tr trends, but estimates of measured were poor for certain sub-treatments, such as FSL and FDH (Fig. 4c).

Measured cumulative Tr variation among treatments for the early season interval in 2003 (Fig. 5a) was similar to that in 2002, where measured Tr varied due to plant density, but not for irrigation or nitrogen treatment. Compared to the 2002 cotton experiment, the differential irrigation scheduling between NDVI and FAO treatment counterparts was slight (less than 50 mm difference in total seasonal applied irrigation water), except between the NSH and FSH, where NSH received about 130 mm less total water than FSH. As seen in Fig. 5b, measured Tr for the interval from DOY 176 to 190 varied primarily with plant density, except for the evident irrigation treatment difference in measured

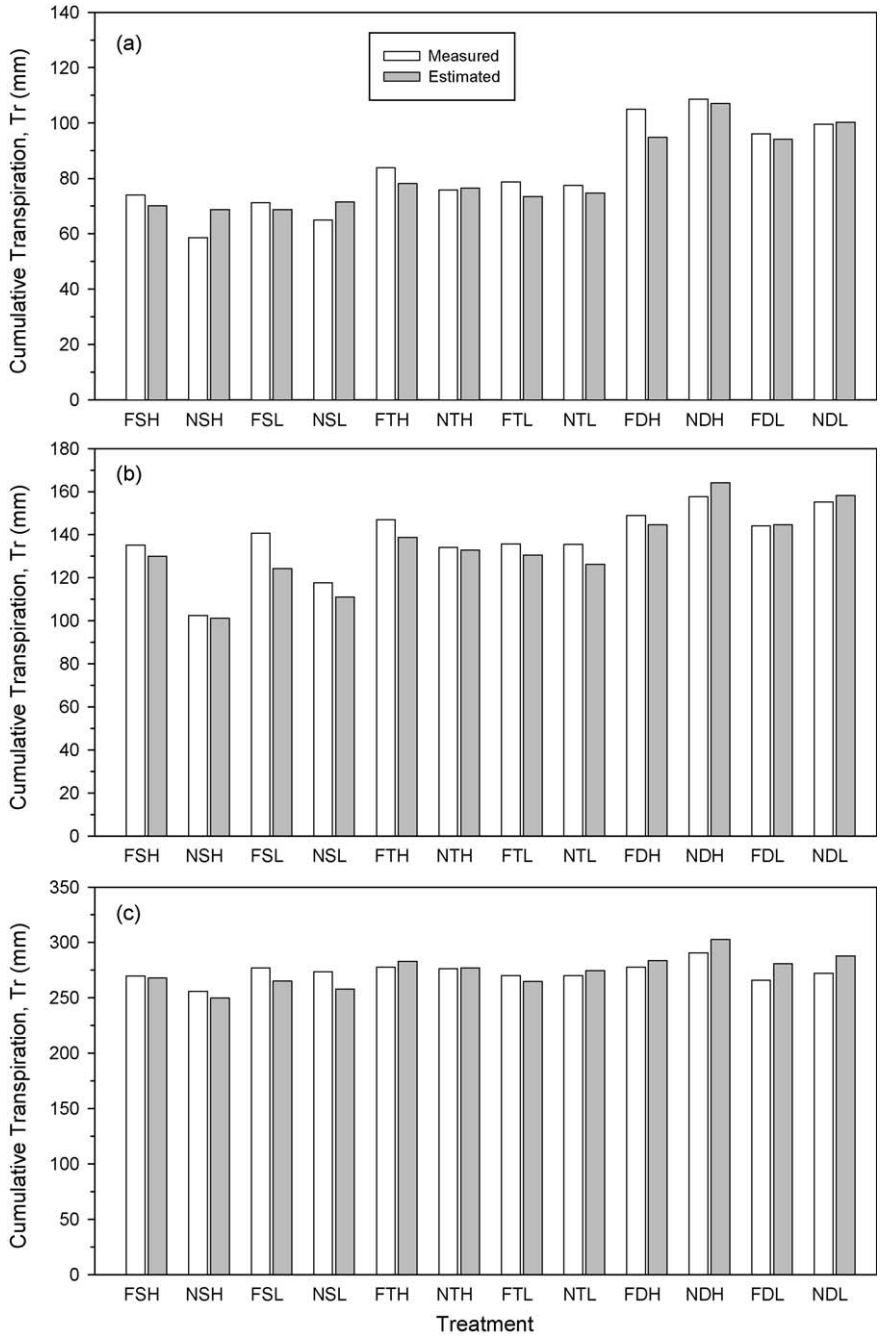

Fig. 5. Means for measured and estimated cumulative transpiration (Tr) for 12 treatments determined for intervals from (a) DOY 153–168, (b) DOY 176–190, and (c) DOY 190–217 in 2003. Measured Tr was determined from soil water balance measurements. Estimated Tr was obtained by multiplying daily Kcb values, derived from imagery-observed NDVI, by daily ETc for all days in a given interval.

Tr between NSH and FSH. However, the interval from DOY 190 to 217, 2003 (Fig. 5c) resulted in more uniform measured Tr among sub-treatments than for the earlier intervals in 2003. For this interval, the effects on measured Tr due to plant density were minimal since most plots were now at full cover, whereas the effects due to N treatment on Tr were not yet evident. The agreement between estimated and measured cumulative Tr appeared reasonably good for most plots in the three intervals of 2003 (Fig. 5a–c).

Summary statistics to aid in evaluating how well the estimated cumulative Tr using ESAP-predicted NDVI agreed with the measured cumulative Tr are provided in Table 7 for the three 2002 intervals and in Table 8 for the three intervals of 2003. For comparison with Tr based on predicted NDVI, statistical summaries are also provided in the tables for the estimated cumulative Tr that used the observed NDVI from imagery.

Excluding the first interval of 2002 (Table 7a), the field-wide means for estimated cumulative Tr were within ±7.8%, 4.0%, 4.6% of the measured field-wide mean for the 6, 12, and 20 sample locations, respectively, which compare favorably with ±3.3% agreement with measured Tr obtained when estimated Tr was based on observed NDVI. In all cases, the field-wide measured mean for the early season interval in 2002 (DOY 163–176) was underestimated, 8.0% based on observed NDVI and 8.6% to 12.5% based on predicted NDVI. As Fig. 4a suggests, underestimation of Tr for the interval was higher for the dense than sparser density treatments, which indicates lower than expected estimated Kcb were obtained for those treatments. The standard deviation for estimated Tr based on predicted NDVI were

Table 7
Mean and standard deviation (SD) for measured and estimated cumulative crop transpiration (Tr) determined for 32 treatment plots over intervals from (a) DOY 163 to 176, (b) DOY 226 to 246, and (c) DOY 246 to 261 during the 2002 cotton growing season. Statistical parameters for estimated Tr include coefficient of determination (r^2), root mean square error (RMSE), mean absolute error (MAE), and mean absolute percent difference (MAPD).

(a) DOY 163–176 (14 days)	Cumulative Tr (mm)					
	Mean	SD				
Measured[a]	88.0	10.7	Statistical parameters for estimated			
Estimated[b]			r^2	RMSE (mm)	MAE (mm)	MAPD (%)
Predicted NDVI, 6 sites	77.0	8.4	0.77	4.1	11.0	12.3
Predicted NDVI, 12 sites	80.4	8.9	0.78	4.3	7.9	8.8
Predicted NDVI, 20 sites	79.3	8.3	0.78	4.1	8.8	9.8
Observed NDVI	81.0	7.9	0.81	3.5	6.7	7.3
(b) DOY 226–246 (21 days)	Cumulative Tr (mm)					
	Mean	SD				
Measured	161.7	14.0	Statistical parameters for estimated			
Estimated			r^2	RMSE (mm)	MAE (mm)	MAPD (%)
Predicted NDVI, 6 sites	161.3	11.6	0.57	7.8	7.5	4.8
Predicted NDVI, 12 sites	162.5	13.4	0.53	9.3	8.3	5.3
Predicted NDVI, 20 sites	162.8	11.4	0.56	7.6	7.6	4.9
Observed NDVI	162.2	16.9	0.75	8.3	6.0	3.7
(c) DOY 246–261 (16 days)	Cumulative Tr (mm)					
	Mean	SD				
Measured	49.8	10.6	Statistical parameters for estimated			
Estimated			r^2	RMSE (mm)	MAE (mm)	MAPD (%)
Predicted NDVI, 6 sites	45.9	10.9	0.59	7.1	6.8	13.0
Predicted NDVI, 12 sites	48.9	13.3	0.60	8.6	6.6	12.7
Predicted NDVI, 20 sites	50.8	15.0	0.60	9.6	6.9	13.4
Observed NDVI	48.4	12.7	0.59	8.2	6.5	12.3

[a] Measured cumulative Tr was determined from soil water balance measurements.
[b] Estimated cumulative Tr was obtained by multiplying the daily Kcb values, derived from NDVI, by the daily ETc for all days in a given interval. The estimated include Tr computed with Kcb based on predicted NDVI using ESAP procedures and 6, 12, and 20 sampling site designs and Tr computed with Kcb based on imagery-observed NDVI.

generally consistent with the SD for measured Tr (within 2 or 3 mm for most intervals). However, the SD for estimated Tr was about 8 mm higher than the measured SD for the last interval of 2003 (Table 8c), indicating greater variability among treatment plots than for measured Tr. Although the SD was closer (within 5 mm) to the measured SD for estimates based on observed than predicted NDVI for the last interval of 2003, SD for observed and predicted were similar for other intervals.

Linear regression of estimated against measured Tr resulted in r^2 values that varied 0.52–0.81, whereas RMSE varied from 4.1 to 12.5 mm (Tables 7 and 8). Generally, the r^2 that were obtained for estimated Tr based on observed NDVI were slightly higher (0.54–0.83), though the RMSE was not consistently lower compared with those based on predicted NDVI. Considering all six intervals, the r^2 values were higher for the shorter (14–16 days) than for the longer (21–28 days) intervals. However, for all regressions considered in the tables, the resultant r^2 were highly significant ($p < 0.01$).

Since the mean and SD for measured cumulative Tr varied among the different intervals, the mean absolute error and the mean absolute percent difference were calculated to provide additional criteria with which to evaluate how well the estimations agreed with the measured cumulative Tr. When cumulative Tr was estimated using the observed NDVI, the MAPD varied from 3.0% to 7.3% for all intervals, excluding the late season interval from DOY 246 to 261 in 2002 where MAPD was 12.3% (Table 7c). The MAPD results for the estimated Tr based on predicted NDVI were generally larger than for those for the observed for each interval, but not appreciably greater (Tables 7 and 8). Excluding the last interval for 2002, the MAPD for the 6, 12, and 20 sample designs for all other intervals were 3.6 to 12.3%, 3.4 to 8.8%, and 3.5 to 9.8%, respectively. The six sample designs had a higher MAPD for the first interval in 2002 (12.3%), but otherwise the MAPD for the six designs were in line with the other two sample designs. The MAPD for the late season interval of 2002 for 6, 12, and 20 sample designs (12.7–13.4%), were similar to the MAPD for the observed for that interval (Table 7c).

The reasons for the poorer agreement between estimated and measured Tr for the late cotton season interval of 2002 than for the other intervals are likely twofold. First, there is a change in the canopy architecture from that during mid-season due to senescing leaves. This can have a large influence on NDVI readings, which may not be closely related to transpiration. Since the relationship between Kcb and NDVI established for the primary cotton growing season models Kcb poorly during the senescence period, a second Kcb-NDVI function was developed to provide a better fit for late season conditions (Hunsaker et al., 2005). Unfortunately, the data used to derive the secondary function was rather limited, thereby resulting in an inexact relationship. Thus, for the late season interval of 2002, which occurred during senescence, the use of the secondary function to calculate cumulative Tr added imprecision to the estimates. However, 12–13% MAPD for estimated Tr, as obtained for the late 2002 interval, could be sufficient for irrigation scheduling purposes late in the cotton season when few if any irrigations are needed.

The results of the evaluations presented above indicate that using ESAP to calibrate and predict the NDVI-basal crop coefficients can be an effective method to estimate the spatial distribution of cotton transpiration within an irrigated field. It was found that the ESAP predicted NDVI provided estimates of measured cumulative Tr, determined from soil water balance

Table 8
Mean and standard deviation (SD) for measured and estimated cumulative crop transpiration (Tr) determined for 32 treatment plots over intervals from (a) DOY 153 to 168, (b) DOY 176 to 190, and (c) DOY 190 to 217 during the 2003 cotton growing season. Statistical parameters for estimated Tr include coefficient of determination (r^2), root mean square error (RMSE), mean absolute error (MAE), and mean absolute percent difference (MAPD).

(a) DOY 153–168 (16 days)	Cumulative Tr (mm)					
	Mean	SD				
Measured[a]	81.9	14.3	Statistical parameters for estimated			
Estimated[b]			r^2	RMSE (mm)	MAE (mm)	MAPD (%)
Predicted NDVI, 6 sites	79.2	10.5	0.78	4.9	6.4	7.5
Predicted NDVI, 12 sites	78.6	9.0	0.78	4.2	6.8	8.0
Predicted NDVI, 20 sites	78.1	12.8	0.81	5.7	5.7	6.7
Observed NDVI	80.1	12.3	0.83	5.2	5.0	6.4
(b) DOY 766–190 (15 days)	Cumulative Tr (mm)					
	Mean	SD				
Measured	137.9	14.1	Statistical parameters for estimated			
Estimated			r^2	RMSE (mm)	MAE (mm)	MAPD (%)
Predicted NDVI, 6 sites	134.1	18.3	0.75	9.2	7.4	5.3
Predicted NDVI, 12 sites	134.5	17.2	0.75	8.7	6.9	5.0
Predicted NDVI, 20 sites	133.0	16.7	0.75	8.4	7.2	5.2
Observed NDVI	133.4	16.3	0.79	7.6	6.8	4.9
(c) DOY 190–217 (28 days)	Cumulative Tr (mm)					
	Mean	SD				
Measured			Statistical parameters for estimated			
Estimated	273.2	9.6	r^2	RMSE (mm)	MAE (mm)	MAPD (%)
Predicted NDVI, 6 sites	270.7	17.7	0.52	12.5	9.8	3.6
Predicted NDVI, 12 sites	272.6	16.7	0.52	11.8	9.2	3.4
Predicted NDVI, 20 sites	271.3	17.4	0.52	12.3	9.6	3.5
Observed NDVI	274.6	14.8	0.54	10.2	8.2	3.0

[a] Measured cumulative Tr was determined from soil water balance measurements.
[b] Estimated cumulative Tr was obtained by multiplying the daily Kcb values, derived from NDVI, by the daily ETc for all days in a given interval. The estimated include Tr computed with Kcb based on imagery-observed NDVI for comparison with Tr computed with Kcb based on predicted NDVI using ESAP procedures and 6, 12, and 20 sampling location designs.

measurements, consistent with estimates obtained using actual NDVI imagery. The measured cumulative transpiration values for 32 plots within the field could be estimated within an absolute mean difference of less then 10%, for all intervals studies, except for the late season period (12–13%) when the cotton was senescing. Thus, the Kcb-NDVI used in conjunction with several well-timed aerial imagery acquisitions of NDVI during the cotton growing season could provide an improvement over traditional methods for managing crop water use and irrigation schedules in spatially variable, surface-irrigated cotton. Depending on the particular irrigation management criteria, field-wide uncertainties for cumulative Tr on the order of 10% or less might or might not be acceptable.

4. Conclusions

- Using sample sizes of 6, 12, and 20 locations, the ESAP software was able to reliably estimate NDVI calibration models for all six prediction dates. The models accurately estimated observed NDVI field means (typically less than 3% difference) and reasonably predicted the observed NDVI standard deviation, though lower than observed standard deviations occurred for all cases.
- When considering all six prediction dates studied, there was not a notable advantage to using more than six sampling locations for predicting spatially distributed NDVI.
- Using ESAP to calibrate and predict the NDVI-basal crop coefficients can be an effective method to estimate the spatial distribution of cotton transpiration within an irrigated field.
- NDVI predicted NDVI provided estimates of measured cumulative Tr, determined from soil water balance measurements, consistent with estimates obtained using actual NDVI imagery.
- Mean absolute point-to-point errors associated with using crop coefficients based on predicted NDVI to estimate cumulative Tr varied from 3.4% to 13.4%, where the higher errors occurred during the end of the season, when the cotton was senescing.
- The Kcb-NDVI used in conjunction with several well-timed aerial imagery acquisitions of NDVI during the cotton growing season could provide an improvement over traditional methods for managing crop water use and irrigation schedules in spatially variable, surface-irrigated cotton.

References

Allen, R.G., Pereira, L.S., Raes, D., Smith, M., 1998. Crop evapotranspiration. FAO Irrigation and Drainage Paper 56. Rome, Italy.
Brown, P.W., 1989. Accessing the Arizona Meteorological Network (AZMET) by computer. Ext. Rep. No. 8733. The University of Arizona, Tucson, AZ, U.S.A.
Chang, J., Clay, D.E., Carlson, C.G., Clay, S.A., Malo, D.D., Berg, R., Kleinjan, J., Wiebold, W., 2003. Different techniques to identify management zones impact nitrogen and phosphorus sampling variability. Agron. J. 95, 1550–1559.
Er-Raki, S., Chehbouni, A., Guemouria, N., Duchemin, B., Ezzahar, J., Hadria, R., 2007. Combining FAO-56 model and ground-based remote sensing to estimate water consumptions of wheat crops in a semi-arid region. Agric. Water Manage. 87, 41–54.
Fitzgerald, G.J., Lesch, S.M., Barnes, E.M., Luckett, W.E., 2006. Directed sampling using remote sensing with a response surface sampling design for site-specific agriculture. Comput. Electron. Agric. 53, 98–112.
Fleming, K.L., Westfall, D.G., Bausch, W.C., 2000. Evaluating management zone technology and grid soil sampling for variable rate nitrogen application. In: Robert, P.C., Rust, R.H., Larson, W.E. (Eds.), Proceedings of the 5th International

Conference on Precision Agriculture, 16–19 July 2000, Bloomington, MN, U.S.A. ASA, CSSA, and SSSA, Madison, WI, CD-ROM, unpaginated.
Gonzalez-Dugo, M.P., Mateos, L., 2008. Spectral vegetation indices for benchmarking water productivity of irrigated cotton and sugarbeet crops. Agric. Water Manage. 95, 48–58.
Hunsaker, D.J., Barnes, E.M., Clarke, T.R., Fitzgerald, G.J., Pinter, P.J., 2005. Cotton irrigation scheduling using remotely sensed and FAO-56 basal crop coefficients. Transactions of ASAE 48 (4), 1395–1407.
Kustas, W.P., Zhan, X., Jackson, T.J., 1999. Mapping surface energy flux partitioning at large scales with optical and microwave remote sensing data from Washita '92. Water Res. Res. 35 (1), 265–277.
Legates, D.R., McCabe, G.J., 1999. Evaluating the 'goodness-of-fit' measures in hydrologic and hydroclimatic model validation. Water Res. Res. 35 (1), 233–241.
Lesch, S.M., 2005. Sensor-directed response surface sampling designs for characterizing spatial variation in soil properties. Comput. Electron. Agric. 46, 153–179.
Lesch, S.M., Strauss, D.J., Rhoades, J.D., 1995. Spatial prediction of soil salinity using electromagnetic induction techniques 1. Statistical prediction models: a comparison of multiple linear regression and cokriging. Water Resources Res. 31 (2), 373–386.
Lesch, S.M., Rhoades, J.D., Corwin, D.L., 2000. ESAP-95 Version 2.01R: User Manual and Tutorial Guide. Research Rpt. 146. USDA-ARS, George E. Brown, Jr., Salinity Laboratory, Riverside, CA, U.S.A.
Moran, M.S., Inoue, Y., Barnes, E.M., 1997. Opportunities and limitations for image-based remote sensing in precision crop management. Remote Sensing Environ. 61, 319–346.
Peters, R.T., Evett, S.R., 2007. Spatial and temporal analysis of crop conditions using multiple canopy temperature maps created with center-pivot-mounted infrared thermometers. Transact. ASABE 50 (3), 919–927.
Pinter, P.J., Hatfield, J.L., Schepers, J.S., Barnes, E.M., Moran, M.S., Daughtry, C.S., Upchurch, D.R., 2003. Remote sensing for crop management. Photogrammetric Eng. Remote Sensing 69 (6), 647–664.
Sadler, E.J., Evans, R.G., Buchleiter, G.W., King, B.A., Camp, C.R., 2000. Design considerations for site specific management. In: Evans, R.G., Benham, B.L., Trooien, T.P. (Eds.), Proceedings of 4th Decennial National Irrigation Symposium, 14–16 November 2000, Phoenix, AZ, U.S.A. ASAE, St. Joseph, MI, U.S.A., pp. 304–315.
Scotford, I.M., Miller, P.C.H., 2004. Estimating tiller density and leaf area index of winter wheat using spectral reflectance and ultrasonic sensing techniques. Biosyst. Eng. 89 (4), 395–408.
Sui, R., Thomasson, J.A., Hanks, J., Wooten, J., 2008. Ground-based sensing system for weed mapping in cotton. Comput. Electron. Agric. 60, 31–38.
Trout, T.J., Johnson, L.F., Gartung, J., 2008. Remote sensing of canopy cover in horticultural crops. HortScience 43 (2), 333–337.
Wood, G.A., Taylor, J.C., Godwin, R.J., 2003. Calibration methodology for mapping within-field crop variability using remote sensing. Biosyst. Eng. 84 (4), 409–423.